

Ponatinib Inhibits Polyclonal Drug-Resistant KIT Oncoproteins and Shows Therapeutic Potential in Heavily Pretreated Gastrointestinal Stromal Tumor (GIST) Patients

Andrew P. Garner¹, Joseph M. Gozgit¹, Rana Anjum¹, Sadanand Vodala¹, Alexa Schrock¹, Tianjun Zhou¹, Cesar Serrano², Grant Eilers², Meijun Zhu², Julia Ketzer³, Scott Wardwell¹, Yaoyu Ning¹, Youngchul Song¹, Anna Kohlmann¹, Frank Wang¹, Tim Clackson¹, Michael C. Heinrich⁴, Jonathan A. Fletcher², Sebastian Bauer³, and Victor M. Rivera¹

Abstract

Purpose: KIT is the major oncogenic driver of gastrointestinal stromal tumors (GIST). Imatinib, sunitinib, and regorafenib are approved therapies; however, efficacy is often limited by the acquisition of polyclonal secondary resistance mutations in KIT, with those located in the activation (A) loop (exons 17/18) being particularly problematic. Here, we explore the KIT-inhibitory activity of ponatinib in preclinical models and describe initial characterization of its activity in patients with GIST.

Experimental Design: The cellular and *in vivo* activities of ponatinib, imatinib, sunitinib, and regorafenib against mutant KIT were evaluated using an accelerated mutagenesis assay and a panel of engineered and GIST-derived cell lines. The ponatinib–KIT costructure was also determined. The clinical activity of ponatinib was examined in three patients with GIST previously treated with all three FDA-approved agents.

Results: In engineered and GIST-derived cell lines, ponatinib potently inhibited KIT exon 11 primary mutants and a range of secondary mutants, including those within the A-loop. Ponatinib also induced regression in engineered and GIST-derived tumor models containing these secondary mutations. In a mutagenesis screen, 40 nmol/L ponatinib was sufficient to suppress outgrowth of all secondary mutants except V654A, which was suppressed at 80 nmol/L. This inhibitory profile could be rationalized on the basis of structural analyses. Ponatinib (30 mg daily) displayed encouraging clinical activity in two of three patients with GIST.

Conclusion: Ponatinib possesses potent activity against most major clinically relevant KIT mutants and has demonstrated preliminary evidence of activity in patients with refractory GIST. These data strongly support further evaluation of ponatinib in patients with GIST. *Clin Cancer Res*; 20(22); 5745–55. ©2014 AACR.

Introduction

Gastrointestinal stromal tumors (GIST) arise primarily through constitutive activation of the receptor tyrosine kinases KIT or platelet-derived growth factor receptor

(PDGFR)A, with approximately 75% of GISTs harboring gain-of-function mutations in KIT (1, 2). These primary activating mutations generally cluster into hotspots within KIT exons 9 and 11. Exon 9 encodes a portion of the extracellular domain, and mutations in this region induce a conformation that mimics that stimulated by ligand binding. The more prevalent exon 11 mutations function by disrupting the secondary structure of the autoinhibitory juxtamembrane domain, thus favoring adoption of the active kinase conformation (3).

The discovery that the tyrosine kinase inhibitor (TKI) imatinib inhibits KIT (4, 5), and its introduction as a treatment (6), transformed the clinical management of GIST. Nonetheless, most imatinib-treated patients ultimately relapse due to outgrowth of clones with secondary, drug-resistant KIT mutations (7, 8). Secondary mutations typically occur in the ATP-binding pocket encoded by exons 13 and 14, and the activation loop (A-loop) encoded by exons 17 and 18 (9). The challenge of treating imatinib-resistant

¹ARIAD Pharmaceuticals, Inc., Cambridge, Massachusetts. ²Department of Pathology, Brigham and Women's Hospital, Harvard Medical School, Boston, Massachusetts. ³Sarcoma Center, Department of Medical Oncology, West German Cancer Center, University of Duisburg-Essen, Essen, Germany. ⁴Portland VA Medical Center and OHSU Knight Cancer Institute, Portland, Oregon.

Note: Supplementary data for this article are available at Clinical Cancer Research Online (<http://clincancerres.aacrjournals.org>).

A.P. Garner and J.M. Gozgit contributed equally to this article.

Corresponding Author: Victor M. Rivera, Preclinical and Translational Research, ARIAD Pharmaceuticals, Inc., 26 Landsdowne St, Cambridge, MA 02139. Phone: 617-494-0400; Fax: 617-225-2589; E-mail: victor.rivera@ariad.com

doi: 10.1158/1078-0432.CCR-14-1397

©2014 American Association for Cancer Research.

Translational Relevance

KIT inhibitors such as imatinib, sunitinib, and regorafenib are effective gastrointestinal stromal tumor (GIST) therapies, although most patients develop resistance to these drugs due to somatic acquisition of polyclonal secondary KIT mutants. The lack of efficacy of any single agent against the complete set of potential ATP-binding pocket and activation loop (A-loop) secondary mutants makes achievement of prolonged complete disease control in late-stage patients challenging. This study demonstrates that ponatinib, a multitargeted tyrosine kinase inhibitor, is a highly potent inhibitor of a broad range of primary and secondary KIT mutants, including those within the A-loop, at clinically achievable concentrations. Clinical use of ponatinib in three patients with refractory GIST demonstrated encouraging antitumor activity. A phase II study of ponatinib for drug-resistant GIST (NCT01874665) is underway.

GISTs is compounded by mutational heterogeneity, as patients can harbor multiple different secondary mutations in distinct tumor lesions, or even within different regions of the same lesion (8).

Patients with GIST with imatinib-resistant tumors are treated with sunitinib, which potently inhibits KIT ATP pocket mutants (10). However, sunitinib is ineffective against A-loop mutants, which account for 50% of imatinib-resistant mutations (11, 12). This may explain why overall response rates (ORR) are low (7%) and median progression-free survival (PFS) is short (6.2 months; refs. 10, 11). Regorafenib was recently approved as third-line therapy but shows only moderate activity, with ORR of 4.5% and median PFS of 4.8 months (13). The KIT-inhibitory properties of regorafenib have not yet been analyzed extensively, but both clinical and initial preclinical data suggest a limited spectrum of sensitive KIT mutants (14, 15). Thus, additional agents are needed to overcome resistance mutations in KIT, in particular those in the A-loop.

Ponatinib (AP24534) is a recently approved BCR-ABL inhibitor that is highly active in heavily pretreated patients with Philadelphia-positive leukemia (16, 17). Ponatinib has a pan-BCR-ABL inhibitory profile in cellular assays, with no single mutation able to confer resistance (18). Ponatinib has also been shown to inhibit select variants of KIT (18, 19). Using cancer cell lines and engineered isogenic mechanistic models, this report describes the preclinical activity of ponatinib against a wide array of KIT mutants and the clinical activity of ponatinib in 3 heavily pretreated patients with GIST.

Materials and Methods

Reagents

Ba/F3 cell lines (DSMZ; ref. 20) and GIST-derived cell lines (21) were cultured as described previously. Mouse Ba/

F3 lines were confirmed using species-specific PCR by the cell bank and were cultured for less than 6 months (further cell line authentication was not conducted). GIST lines were routinely monitored by Sanger sequencing and SNP profiling to confirm their *KIT* mutation status and cell line identity.

KIT cDNAs were synthesized in pLVX-IRES-puro (Clontech) by GenScript. Lentiviral particles were generated using a Trans-lentiviral ORF packaging kit (Thermo Scientific).

Antibodies against KIT, phospho-KIT(Tyr⁷²¹), ERK, phospho-ERK(Thr²⁰²/Tyr²⁰⁴), AKT, and phospho-AKT(S⁴⁷³) were obtained from Cell Signaling Technologies.

Ponatinib was synthesized at ARIAD Pharmaceuticals and imatinib (OntarioChem), sunitinib, and regorafenib (Selleck Chemicals) obtained from commercial vendors (Supplementary Fig. S1).

Generation of Ba/F3 stable cell lines

KIT cDNA was cloned into the pLVX-IRES-Puro vector (Clontech) and Ba/F3 cells infected with lentiviral particles. Cells expressing KIT were selected by IL3 (R&D Systems) withdrawal and puromycin (0.5–1 µg/mL, Invitrogen). Native KIT cells were grown in the presence of mouse Stem Cell Factor (mSCF) (20 ng/mL; Life Technologies).

Viability assays

Cell lines were plated at densities that produced linear growth, treated with 8 concentrations of drug, and viability assessed using CellTiter-96 Aqueous One (Promega) after 72 hours. Data were plotted as percentage of viability relative to vehicle-treated cells and IC₅₀ values calculated using XLfit.

Immunoblotting

Approximately 120 µg of clarified protein lysates (RIPA buffer) was subjected to Western blotting using KIT primary antibodies, horseradish peroxidase-conjugated secondary antibodies (Cell Signaling Technology) and the signal visualized with SuperSignal West Femto Substrate (Thermo Scientific).

Mutagenesis screen

Ba/F3 cells containing a single copy of *KIT* exon 11(Δ557–558) were treated overnight with *N*-ethyl-*N*-nitrosourea (50 µg/mL). Cells were seeded in flasks with various concentrations of compound and outgrowth monitored. Resistant cells were harvested, the *KIT* kinase domain PCR-amplified and analyzed by next-generation sequencing (MolecularMD).

In vivo studies

All animal experiments were carried out under a protocol approved by the Institutional Animal Care and Use Committee. Tumors were established by subcutaneous implantation of engineered Ba/F3 or GIST-derived cell lines into CB.17/SCID mice (Charles River Laboratories) or the GIST-1 patient-derived tumor (PDX) into NOD/SCID mice

(Molecular Response); both strains female and 8 to 9 weeks old. The GIST-1 PDX contained a KIT exon 11(Δ 557–558) primary mutation and Y823D secondary mutation.

For efficacy studies, mice were randomized to treatment groups when the average tumor volume reached about 200 mm³. Mice were treated once daily by oral gavage with compound or vehicle (water for imatinib, 25 mmol/L citrate buffer for ponatinib and sunitinib and NMP/PEG400 for regorafenib). The mean tumor volume of the treatment group was divided by that of the control group (at final measurement) to calculate percentage of tumor growth inhibition. For pharmacodynamic studies, tumor-bearing mice were treated with a single dose of compound for 2 hours. Tumors were harvested and protein lysates prepared for Western blotting.

Crystallography

KIT cloning, protein expression, and purification were performed as described previously (22). Ponatinib was mixed with native KIT protein (3:1 molar ratio) and subjected to Glu-C protease treatment (25°C) for 1 hour. A concentrated sample (10 mg/mL) was crystallized at 20°C in 0.1 mol/L Tris-HCl, pH 8.5, 2 mol/L ammonium phosphate monobasic. The complex structure was solved at 2.0 Å resolution by molecular replacement. Model building was performed using Quanta and structural refinement with CNX. The entire inhibitor molecule was well-resolved in the electron density map and the final model possessed good statistics (R factor 20.4% and R-free 23.9%).

Results

Ponatinib is a potent inhibitor of KIT exon 11 primary activating mutants as well as gatekeeper and A-loop secondary mutants

Using *in vitro* kinase assays, we compared ponatinib activity to that of imatinib, sunitinib, and regorafenib (Supplementary Table S1). Consistent with previous data on a smaller set of variants (18), ponatinib potently ($IC_{50} \leq 11$ nmol/L) inhibited native (wild-type) KIT, as well as KIT with mutations within exon 11 (V559D and V560G), at the gatekeeper residue (T670I) and within the A-loop (D816H, D820E, and A829P), although it was less potent against V654A. Ponatinib had at least an order of magnitude greater potency against A-loop mutants than imatinib, sunitinib, and regorafenib.

To assess the cellular KIT activity of each inhibitor, we generated a comprehensive panel of Ba/F3 cell lines whose viability was KIT-dependent (Supplementary Table S2). KIT expression and phosphorylation were confirmed in these lines (Supplementary Fig. S2). Despite the variable KIT expression and phosphorylation levels observed, growth rates across the panel were broadly comparable (data not shown).

We first examined the activity of each compound against 6 cell lines containing primary activating mutations in KIT (Fig. 1A and Supplementary Table S3). The panel included mutants representative of the most common categories of

activating mutations, that is, in-frame exon 11 deletions (Δ 550–557, Δ 551–554, Δ 557–558), as well as a point mutation (V560D) and insertion/deletion (K558NP) within exon 11, and an insertion within exon 9 (502AY). Activity against native KIT was also examined. Imatinib and regorafenib were effective inhibitors of all KIT exon 11 primary mutants tested ($IC_{50} \leq 30$ nmol/L), except Δ 551–554 (IC_{50} , 90–141 nmol/L), but these drugs were less potent versus the exon 9 mutant ($IC_{50} > 130$ nmol/L). Sunitinib was a potent inhibitor of all KIT exon 11 and exon 9 primary mutants tested ($IC_{50} \leq 7$ nmol/L), except Δ 551–554 (IC_{50} , 42 nmol/L). Ponatinib potently inhibited all KIT exon 11 mutants tested, including Δ 551–554 ($IC_{50} \leq 15$ nmol/L) and had the lowest IC_{50} against each. However, the potency of ponatinib toward the exon 9 mutant was reduced (IC_{50} , 56 nmol/L). The activity of all TKIs against exon 9 mutant KIT was similar to their activity against native KIT (Fig. 1A), which is consistent with their intracellular domains being wild-type.

To confirm that inhibition of cell viability was due to inhibition of KIT, we assessed KIT Y721 phosphorylation in inhibitor-treated cells (Supplementary Fig. S3). The results were supportive of the viability data, with phosphorylation levels of KIT exon 11 mutants being sensitive to all inhibitors tested. In contrast, KIT exon 9 mutant phosphorylation was less sensitive to ponatinib, imatinib, and regorafenib. In addition, all inhibitors tested displayed substantially reduced potency against parental Ba/F3 cells grown in the presence of IL3 ($IC_{50} > 2$ μ mol/L; Supplementary Table S3), further demonstrating their selectivity for KIT in this system.

The impact of secondary kinase domain mutations on each inhibitor was next assessed in the context of one of the major primary KIT mutants, exon 11 Δ 557–558 (Fig. 1B and C and Supplementary Table S3). Imatinib potency was severely reduced in the presence of secondary ATP pocket (V654A and T670I) and A-loop mutants (D816H/G, D820A/G, N822K, and A829P) with IC_{50} values ranging from 170 to 10,000 nmol/L. Sunitinib effectively overcame ATP pocket ($IC_{50} \leq 12$ nmol/L), but not A-loop mutants ($IC_{50} > 204$ nmol/L). In contrast, secondary mutations within the A-loop, or at the gatekeeper (T670I) residue, only had a modest impact on ponatinib potency ($IC_{50} \leq 13$ nmol/L). Consistent with the *in vitro* kinase data, the V654A mutation led to a more pronounced (20-fold) decrease in ponatinib potency. The profile of regorafenib was qualitatively similar to that of ponatinib, although its potency was substantially reduced relative to ponatinib in all cases. TKI potency, as measured by inhibition of KIT phosphorylation, was consistent with that observed for cell viability (Supplementary Fig. S3). These findings were confirmed by analysis of imatinib, sunitinib, and ponatinib sensitivity of a similar panel of secondary resistance mutants in a KIT exon 11–mutant backbone using an isogenic, CHO transient transfection model (data not shown; ref. 23).

To extend our analysis, the effects of V654A and D816H secondary mutations were also studied in the context of exon 9 insertion and exon 11 V560D primary mutations

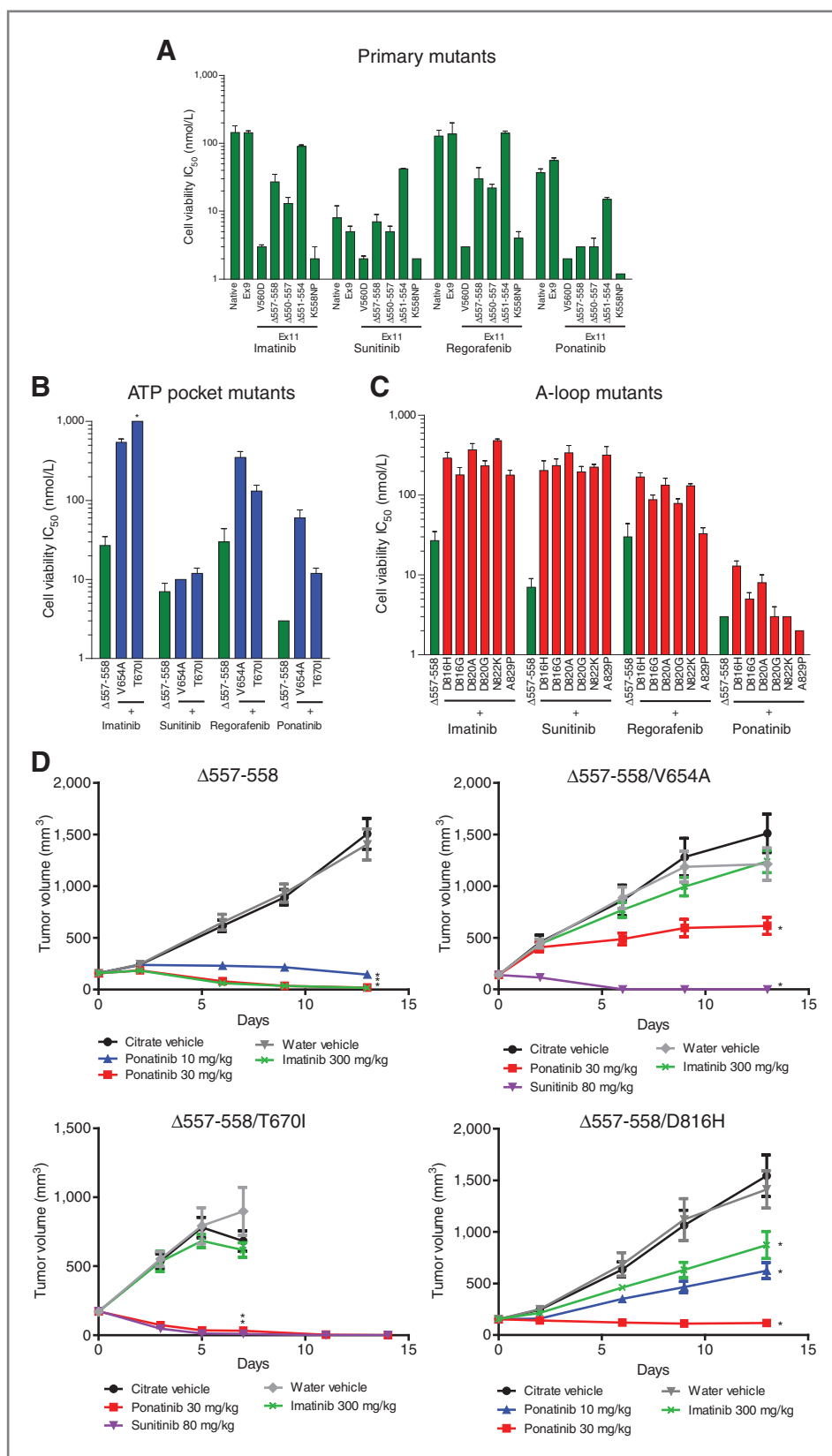


Figure 1. Ponatinib potently inhibits a broad spectrum of KIT primary activating and secondary resistance mutants *in vitro* and *in vivo*. IC₅₀ values (nmol/L) of imatinib, sunitinib, regorafenib, and ponatinib in Ba/F3 cells harboring (A) native or primary mutant KIT alone (green bars), (B) exon 11 (Δ557–558) + ATP pocket secondary mutants (blue bars), and (C) exon 11 (Δ557–558) + A-loop secondary mutants (red bars). The cell lines were treated with increasing concentrations of the drug for 3 days followed by cell viability assessment using the MTT assay. Data are shown as mean ± SD from 3 separate experiments. D, *in vivo* efficacy of ponatinib, imatinib, and sunitinib in subcutaneous tumor models using Ba/F3 KIT-mutant cells. Imatinib (300 mg/kg) was used as a comparator to ponatinib (30 mg/kg) in all 4 models. On the basis of *in vitro* potencies, sunitinib was included as a second comparator in 2 models (Δ557–558/V654A and Δ557–558/T670I) in which imatinib was expected to be nonefficacious, and a lower dose of ponatinib (10 mg/kg) was also tested in the Δ557–558 and Δ557–558/D816H models. Tumor-bearing animals were treated once daily by oral gavage with vehicle or the indicated doses of drug for 12 days. Mean tumor volume and SEM are plotted. Each treatment group was compared with the relevant vehicle group using 1-way ANOVA, with statistical significance ($P < 0.05$) indicated by an asterisk.

(Supplementary Fig. S4) and their effects compared with that seen in the context of the exon 11 $\Delta 557$ –558 primary mutation (Fig. 1A–C and Supplementary Table S3). Interestingly, the degree of resistance imparted by V654A or D816H toward all 4 TKIs was consistently most pronounced in the context of V560D primary mutation. This is surprising given that in the absence of a secondary mutation, all 4 TKIs had greatest potency toward V560D versus the other primary mutants.

Ponatinib displays *in vivo* activity in KIT-dependent Ba/F3 models

To examine the effect of ponatinib on the growth of KIT mutant cells *in vivo*, we compared the activity of ponatinib to that of imatinib and/or sunitinib in Ba/F3 cell models implanted in mice (Fig. 1D and Supplementary Table S4). Once daily oral administration of ponatinib had a potent, dose-dependent effect on growth of tumors with a primary KIT exon 11 ($\Delta 557$ –558) mutation alone, with 30 mg/kg inducing near-complete tumor regression that was identical to that obtained with a 10-fold higher dose of imatinib (300 mg/kg). Imatinib had no significant effect on growth of tumors bearing the secondary ATP pocket mutations V654A or T670I, whereas sunitinib (80 mg/kg) induced regressions in both. Ponatinib was only moderately efficacious (65% tumor growth inhibition) in tumors with a V654A mutation but induced complete regression of

tumors with a T670I secondary mutation. Importantly, ponatinib, but not imatinib, induced regression of tumors with the secondary A-loop mutation D816H.

Ponatinib suppresses emergence of A-loop mutations in a cell-based mutagenesis screen

To more broadly assess the potential mutational liabilities of ponatinib, imatinib, sunitinib, and regorafenib, we performed an *in vitro* mutagenesis screen (18). Ba/F3 cells with a primary KIT exon 11 mutation ($\Delta 557$ –558) were mutagenized and incubated with various concentrations of each compound and the KIT mutation status of the resistant cell populations that emerged assessed by next-generation sequencing. With each inhibitor we observed a concentration-dependent reduction in the number of resistant clones that survived (data not shown). Ponatinib, sunitinib, and regorafenib were found to fully suppress the emergence of resistant clones at 80, 500, and 1,000 nmol/L, respectively, whereas resistant clones were still observed at the highest concentration of imatinib tested (1,000 nmol/L; Fig. 2).

Imatinib and regorafenib selected for clones with both ATP pocket (particularly V654A and/or T670I) and A-loop D816 mutations. In contrast, sunitinib primarily selected for outgrowth of a variety of A-loop mutants, with N822K being particularly frequent. The pattern of mutants induced by ponatinib was distinct, with the V654A ATP pocket

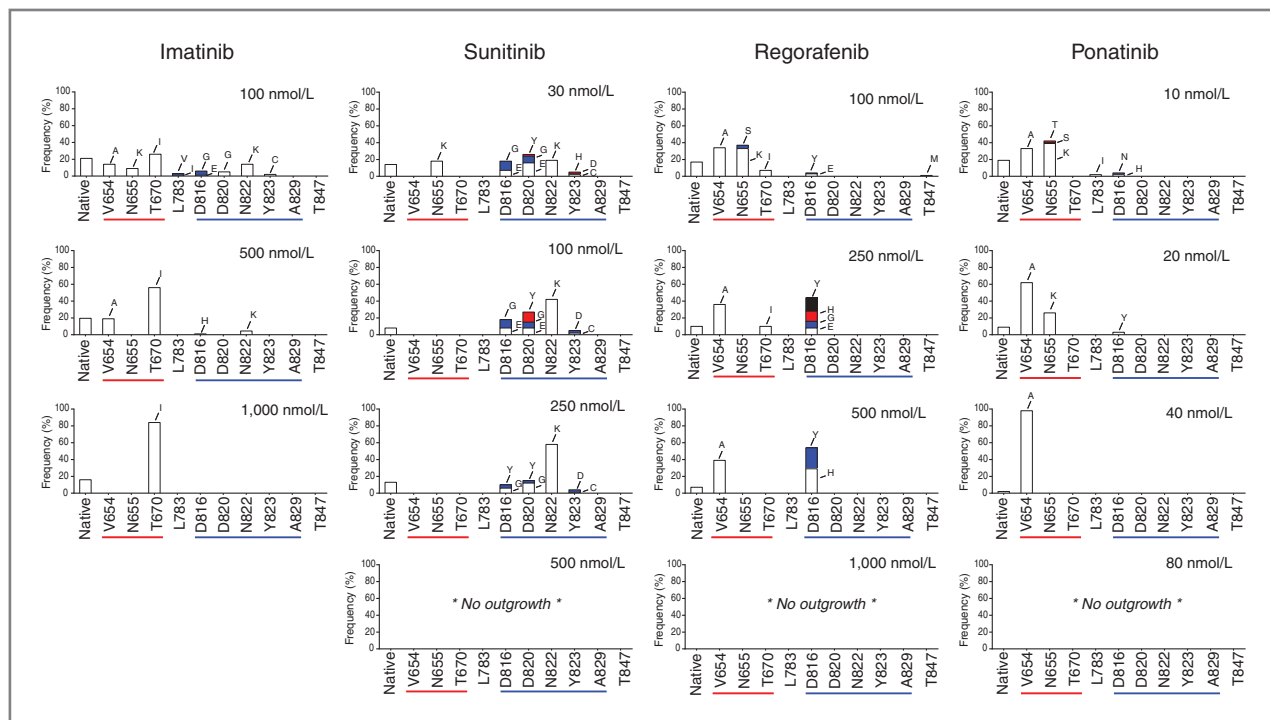


Figure 2. Secondary resistance mutants identified in the presence of KIT inhibitors. Resistant cells were recovered from *N*-ethyl-*N*-nitrosourea-treated Ba/F3 KIT Ex11 ($\Delta 557$ –558) cells and cultured with imatinib, sunitinib, regorafenib, or ponatinib at the indicated concentrations. Each bar represents the relative frequency of the indicated KIT kinase domain secondary mutation, based on next-generation sequencing data. (Reported mutation frequencies are a composite of both mutation incidence and cell number.) ATP pocket residues are underlined in red and A-loop residues in blue. Mutagenesis data are shown from a representative experiment; similar results were obtained in 3 separate studies.

mutant being most prevalent and, importantly, A-loop mutants being observed rarely and only at concentrations below 40 nmol/L.

Among the sites of mutation selected for by ponatinib and regorafenib, virtually all have been previously associated with resistance to imatinib or sunitinib (9, 24). The only exceptions were N655 mutants, especially N655K, which were commonly observed at low doses of all drugs. Characterization of a Ba/F3 cell line with an N655K secondary mutation indicated that it had a relatively minor impact on potency of all 4 TKIs (≤ 5 -fold; Supplementary Table S3).

Structural analysis to explain the KIT selectivity profile of ponatinib

In an effort to rationalize the KIT selectivity profile of ponatinib, a high-resolution (2.0 Å) crystal structure of the KIT kinase domain in complex with ponatinib was determined (pdb code: 4U0I) and compared with apo KIT and imatinib- and sunitinib-KIT costructures (22, 25).

Ponatinib simultaneously occupies 3 pockets within KIT (ATP, selectivity, and DFG; Fig. 3A) and induces the KIT-inactive (DFG-out) conformation, with the juxtamembrane domain disengaged from the kinase active site. Although imatinib has a similar overall binding mode, ponatinib makes additional molecular contacts in both the ATP and DFG pockets that likely explain its increased affinity for KIT (Supplementary Fig. S5). Sunitinib, on the other hand, primarily occupies the ATP pocket and not the DFG pocket, which remains occupied by the juxtamembrane domain.

The interactions between ponatinib and the DFG pocket may explain the relative sensitivities of different primary KIT mutants (Fig. 1A and Supplementary Table S3). W557 of the autoinhibitory juxtamembrane domain occupies the DFG pocket in the apo form but is displaced when ponatinib is bound (Fig. 3B). The need for ponatinib to competitively displace W557 is consistent with the relatively high IC_{50} of ponatinib against native and exon 9 mutant KIT, compared with the 10-fold lower IC_{50} against forms in which W557 is deleted ($\Delta 550-557$ and $\Delta 557-558$). Likewise, the high potency of ponatinib against V560D and K558NP primary mutants is consistent with the prediction that these mutations disrupt hydrophobic or hydrogen bond interactions between the juxtamembrane domain and the kinase domain, facilitating displacement of W557 by ponatinib. A similar rationale and trend of inhibitor activity also applies to the DFG-out inhibitor imatinib. In contrast, sunitinib, by virtue of not binding to the DFG pocket, is less influenced by the presence of W557, which is consistent with its potent inhibition of native and exon 9 mutant KIT.

With respect to mutations in the ATP pocket, the V654A secondary mutation has a major effect on the potency of ponatinib and imatinib and a minor impact on that of sunitinib (Fig. 1B and Supplementary Fig. S4). V654 forms 6 van der Waals interactions with ponatinib, each with favorable interaction distances (< 4.5 Å), that are predicted to be lost when V654 is replaced by a smaller alanine residue (Fig. 3C). Similarly, a total of 5 molecular contacts are predicted

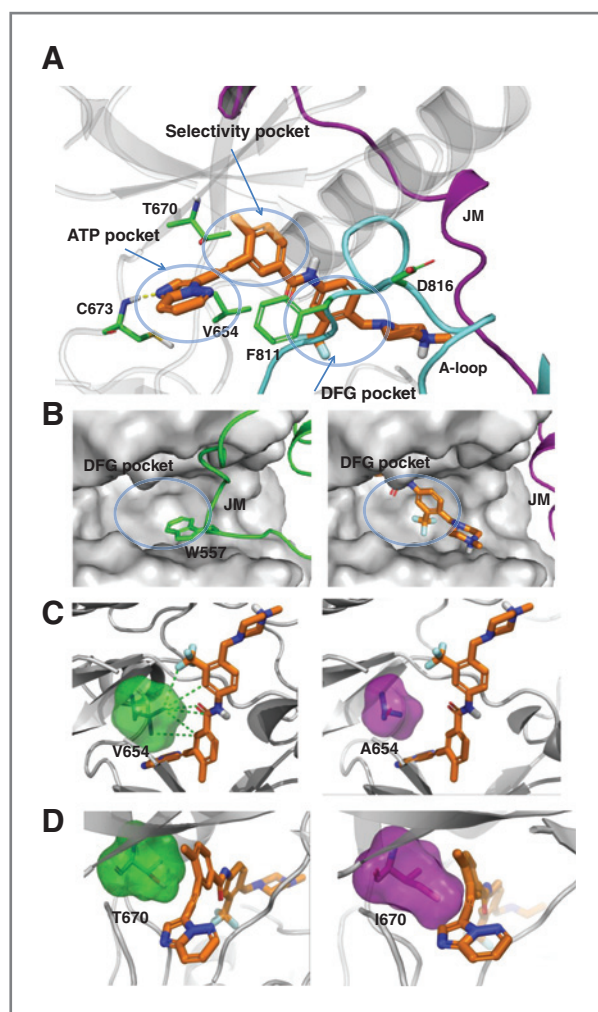


Figure 3. Co-crystal structure of KIT bound with ponatinib. A, crystal structure of ponatinib in complex with the native KIT kinase domain. Ponatinib is shown in gold, side chains of C673 (hinge region) and other key amino acids referred to in the text in green, the A-loop in cyan, and the juxtamembrane (JM) domain in magenta. B, left, W557 of the KIT JM domain (green) occupies the DFG pocket in the apo form. Right, ponatinib (gold) displaces W557 and the JM domain upon binding. C, the impact of V654A mutation on ponatinib binding. Left, the green dashed lines indicate van der Waals contacts between V654 (green) and ponatinib (gold). Right, the mutation of valine to alanine (magenta) results in a loss of all van der Waals contacts with ponatinib. D, illustration of the ability of ponatinib to accommodate the space requirements of T670I gatekeeper mutant. The increase in steric bulk upon mutation from T670 (green, left) to I670 (magenta, right) is accommodated by the triple bond of ponatinib (gold).

to be lost in the case of imatinib. In contrast, analysis of sunitinib bound to KIT suggests a loss of only one van der Waals contact. Despite similar overall binding modes, ponatinib maintains activity against the T670I gatekeeper secondary mutant (Fig. 3D), whereas imatinib does not (Fig. 1B).

Ponatinib is uniquely able to maintain substantial potency in the presence of secondary A-loop mutations, with low IC_{50} values (≤ 13 nmol/L) against all 6 mutants tested

Table 1. Ponatinib IC₅₀ values (nmol/L) in cell lines established from tumor biopsies in patients with GIST

Cell line	KIT status	Ponatinib	Imatinib	Sunitinib	Regorafenib
GIST882	K642E	31	173	54	503
GIST430	Δ560–576	12	61	68	191
GIST430/654	Δ560–576/V654A	159	1,204	90	1,001
GIST430/654/680	Δ560–576/V654A/N680K	330	>5,000	1,314	4,969
GIST-T1	Δ560–578	5	30	15	110
GIST-T1/670	Δ560–578/T670I	8	>5,000	48	249
GIST-T1/816	Δ560–578/D816E	23	604	3,111	395
GIST-T1/829	Δ560–578/A829P	16	1,201	1,168	934
GIST48/820	V560D/D820A	34	413	587	164
GIST48B	KIT-independent	806	>5,000	>5,000	>5,000
GIST226	KIT-independent	2,807	>5,000	3,856	>5,000

(Fig. 1C and Supplementary Table S3). The D816H mutation has the greatest effect on ponatinib potency and confers resistance to all other TKIs tested. D816, located in the middle of the A-loop, forms hydrogen bonds with neighboring residues that stabilize the A-loop conformation. F811, which is located at the beginning of A-loop, makes van der Waals contacts with ponatinib (Fig. 3A) as well as imatinib and sunitinib. Destabilization of the A-loop conformation by the D816H and other A-loop mutations is predicted to disrupt these interactions, with such a disruption having a smaller impact on ponatinib binding due to the overall extended network of optimized contacts ponatinib makes with KIT.

Ponatinib displays activity in *in vitro* and *in vivo* models derived from patients with GIST

To assess the activity of ponatinib and other TKIs in more clinically relevant systems, we determined their impact on KIT-dependent signaling and growth using a panel of KIT-mutant cell lines derived from patients with GIST (Table 1 and Supplementary Fig. S6). Consistent with engineered KIT mutant models, imatinib was selectively active in GIST lines harboring primary KIT exon 11 mutations (GIST430 and GIST-T1), whereas sunitinib also inhibited lines with secondary ATP pocket mutations (GIST430/654 and GIST-T1/670). However, sunitinib had substantially reduced activity in lines harboring secondary A-loop mutations (GIST-T1/816, GIST-T1/820, and GIST-T1/829). In contrast, ponatinib remained highly active in GIST lines harboring secondary A-loop mutations, or a T670I gatekeeper mutation, although its activity was adversely affected by the presence of V654A. The overall inhibition profile for regorafenib was broadly similar to that of ponatinib, although regorafenib was consistently less potent. Little activity was observed in KIT-independent cell lines, confirming the specificity of these findings.

In vivo, a single dose of ponatinib (30 mg/kg) or imatinib (300 mg/kg) significantly inhibited KIT, ERK, and AKT phosphorylation in GIST with a primary exon 11 mutation (GIST430; Fig. 4A). However, in tumors con-

taining a V654A secondary mutation (GIST430/654), both agents had more modest effects on signaling. In a patient-derived xenograft harboring a Y823D A-loop secondary mutation and an exon 11 primary mutation (Δ557–558), a single dose of ponatinib inhibited KIT-driven signaling (Fig. 4A), and once daily dosing rapidly induced complete regression (Fig. 4B). Although imatinib (78% tumor growth inhibition), sunitinib (96% tumor growth inhibition), and regorafenib (75% tumor regression) each exhibited some degree of efficacy during 4 weeks of dosing, ponatinib was the only agent to induce complete regression. Moreover, this complete regression was maintained in all mice for an additional 6 weeks after ponatinib dosing was stopped.

Single-agent ponatinib displays encouraging clinical activity in relapsed patients with GIST

Three refractory patients with GIST, all of whom had been treated previously with, at a minimum, imatinib (both 400 and 800 mg), sunitinib, and regorafenib, were treated with ponatinib, individually, after providing written informed consent (see Supplementary Material for detailed patient information). Patients were treated with 30 mg ponatinib, administered orally once daily, and evaluated by CT scan after 4 weeks of treatment. All patients were known to have had primary *KIT* mutations in exon 11. Notably, ponatinib displayed clinical activity in 2 of the 3 patients.

In patient 1, ponatinib induced a radiologic response in all lesions (Fig. 5A) with ongoing disease control for 6 months. This patient had most recently exhibited rapid progression following salvage treatment with pazopanib. In patient 2, ponatinib induced a mixture of tumor regression and stable disease across the patient's multiple lesions (Fig. 5B). This patient, with multiple cardiovascular risk factors, was treated with ponatinib for a total of 10 weeks, at which point an episode of acute chest pain revealed previously unknown severe coronary artery disease and ponatinib was discontinued. The patient died of myocardial infarction 5 weeks after ponatinib discontinuation. In

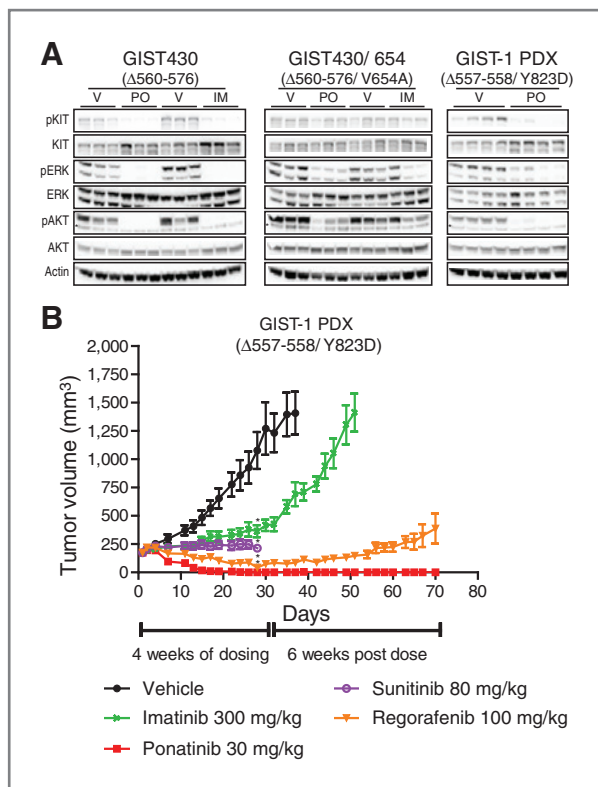


Figure 4. Ponatinib activity in patient-derived KIT-driven tumor models. A, KIT phosphorylation and downstream signaling were evaluated by immunoblot in GIST430, GIST430/654, and GIST-1 PDX-implanted animals treated with a single oral dose of vehicle (V), 30 mg/kg ponatinib (PO), or 300 mg/kg imatinib (IM), $n = 3$ per group. B, *in vivo* efficacy of ponatinib, imatinib, sunitinib, and regorafenib in GIST-1 PDX model. Tumor-bearing animals were treated once daily by oral gavage with vehicle or the indicated dose of drug for the indicated dosing period. Mean tumor volume and SEM are plotted. The vehicle used for ponatinib and sunitinib is shown (citrate buffer); nearly identical tumor growth was observed for the vehicles used for imatinib (water) and regorafenib (NMP/PEG; data not shown). Statistical significance, calculated using one-way ANOVA ($P < 0.05$) in which each treatment group (day 28) was compared to its vehicle control, is indicated by an asterisk. Data are shown for all groups until fewer than 8 of the original 10 mice in each group remained. In the vehicle and imatinib groups, mice were sacrificed when tumors became too large. In the sunitinib treatment group, multiple mice were sacrificed because of $>20\%$ body weight loss.

patient 3, global progression of disease was observed after 4 weeks of ponatinib (Fig. 5C). This patient had also been treated previously with pazopanib.

Discussion

Treatment paradigms and outcomes for patients with GIST and chronic myeloid leukemia (CML) share a number of important features: these neoplasms are generally initiated by oncogenic tyrosine kinases (KIT/PDGFR and ABL, respectively), first-line treatment with the KIT/PDGFR/ABL inhibitor imatinib induces high response rates, and disease progression is commonly associated with acquisition of secondary drug-resistance mutations

in the original kinase target (26). In CML, more potent ABL inhibitors such as dasatinib and nilotinib have been developed that can be effective treatments for patients whose disease becomes resistant to imatinib (27, 28). These agents also induce higher response rates than imatinib in newly diagnosed patients (29, 30) and result in a narrower spectrum of secondary resistance mutants (31). Importantly, these properties were predicted by preclinical studies that demonstrated the superior potency of these agents over imatinib and their ability to inhibit many, although not all, mutations (32). Among the several ABL mutations that confer resistance to dasatinib and nilotinib, the T315I gatekeeper mutation is most notable because it confers resistance to all available therapies. Ponatinib was designed to overcome T315I and other resistance mutations (18). In preclinical studies, ponatinib has the properties of a pan-BCR-ABL inhibitor, that is, no single mutation has been identified that can confer resistance. In a phase II study in heavily pretreated patients, response rates to ponatinib substantially exceeded those achieved on the prior line of treatment (17).

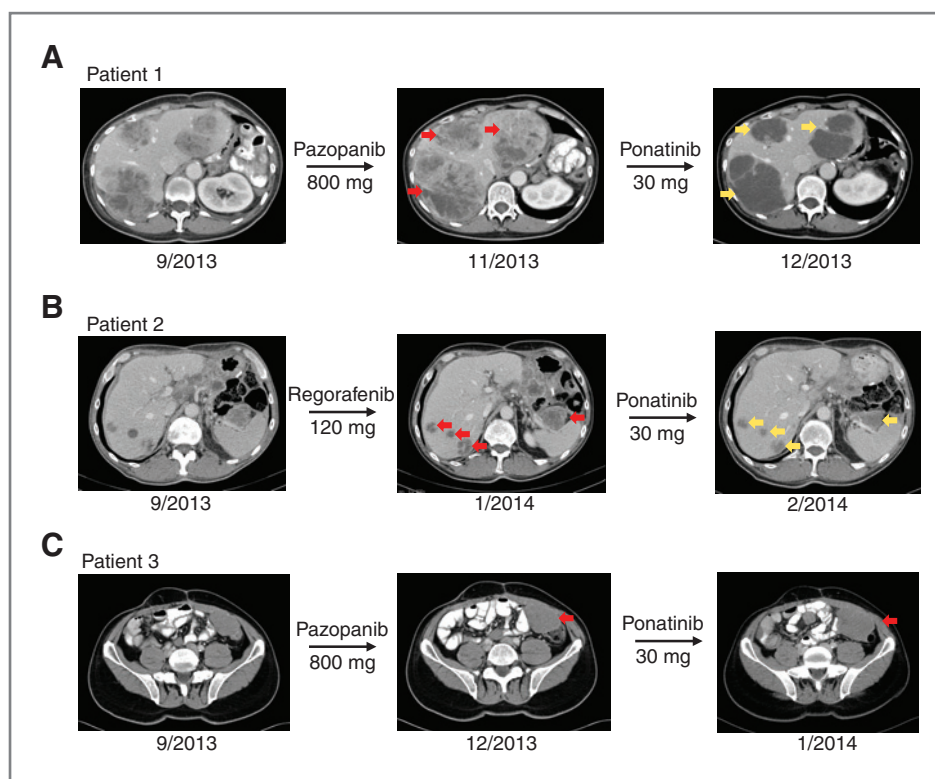
In GIST, however, no TKI has yet demonstrated strong activity in refractory patients, with rates and duration of response being low in patients treated with sunitinib in second-line (11) and regorafenib in third-line (13). As was the case in CML, preclinical profiles of the approved TKIs mirror their clinical profiles. The greater degree of efficacy of imatinib in patients with exon 11 versus exon 9 primary mutations, and the emergence of imatinib-resistant clones with secondary mutations in the ATP pocket and A-loop can all be recapitulated in preclinical models (9). This is also the case for sunitinib, which, for example, has preclinical and clinical activities against imatinib-resistant secondary mutations in the ATP pocket but not the A-loop (10, 12, 24). The challenge of effectively treating refractory GIST is compounded by the heterogeneous nature of secondary mutations that can be observed in patients (33). Thus, there remains a clear need for an agent that can overcome, and potentially suppress emergence of, the broad array of potential resistance mutations in KIT. Furthermore, preclinical models should provide useful guidance to prioritize clinical evaluation of compounds with the desired profile.

Here, we used systematic preclinical models, including *in vitro* kinase assays, cellular and *in vivo* assays, to assess ponatinib activity against the more common clinically relevant primary and secondary KIT mutants in GIST. These studies assessed effects on KIT-driven signaling and tumor growth in 20 engineered Ba/F3 cell lines, 9 cell lines derived from patients with GIST, and a GIST patient-derived tumor model, with consistent results observed across the different model systems. Imatinib, sunitinib, and regorafenib were used as comparators. We also solved the structure of the KIT kinase domain in complex with ponatinib and compared it with available KIT-imatinib and KIT-sunitinib structures to provide mechanistic models for the KIT-inhibitory profile of ponatinib.

Imatinib and sunitinib are clinically effective inhibitors of KIT with primary activating mutations in exon 11 and they potently inhibited such mutants in all of the models

Figure 5. Single-agent ponatinib is active in heavily pretreated patients with TKI-resistant GIST.

Representative CT scans of 3 patients with KIT exon 11-mutant GIST before and after treatment with 30-mg ponatinib for 4 weeks. Each patient was heavily pretreated with imatinib, sunitinib, and regorafenib. A, patient 1: ponatinib induced regression and cyst-like transformation of multiple metastatic lesions. B, patient 2: ponatinib induced moderate responses in multiple lesions. C, patient 3: no response to ponatinib treatment. Red arrows highlight areas of tumor growth, whereas yellow arrows indicate tumor response.



examined in this study. Likewise, ponatinib potently inhibited KIT exon 11 mutants (IC_{50} , 1–15 nmol/L), with potency ranging from comparable to up to 9-fold greater than that of sunitinib and imatinib against all 5 mutants tested in engineered Ba/F3 cells. Regorafenib had similar or somewhat reduced potency compared with that of imatinib and sunitinib. Sunitinib (IC_{50} , 5 nmol/L) was a substantially more potent inhibitor of KIT with an exon 9 insertion than all of the other TKIs, including ponatinib (IC_{50} , 56 nmol/L). The selectivity of ponatinib (as well as imatinib) for exon 11 versus exon 9 mutant KIT can be explained by its need to competitively displace the W557 residue in the auto-inhibitory juxtamembrane domain for optimal binding. This exon 11 residue functions normally in exon 9 mutant KIT but is deleted, or its interaction with KIT impaired, by mutations in exon 11. In contrast, W557 displacement is not required for sunitinib binding. The overall high potency with which ponatinib inhibits exon 11 mutant KIT may be explained by the extensive network of contacts ponatinib makes with KIT through interaction with 3 distinct binding pockets.

The V654A (exon 13) secondary mutation causes resistance to imatinib but not sunitinib. Of all secondary mutants tested, ponatinib was least active against this ATP pocket mutant, with relatively high IC_{50} values (60–101 nmol/L) in 2 different Ba/F3 models. In mice, ponatinib was able to inhibit growth of tumors containing a KIT exon 11 primary mutant and a V654A secondary mutant by 65%, but the same dose induced complete regression of tumors expressing the primary mutant alone. Regorafenib also did

not appear to be an effective inhibitor of this mutant. Structural analysis shows that ponatinib and imatinib, but not sunitinib, make a large number of van der Waals interactions with V654 that are predicted to be lost when this residue is mutated to a smaller alanine residue.

The T670I gatekeeper mutation (exon 14) also causes resistance to imatinib but not sunitinib or ponatinib (IC_{50} , 12 nmol/L), and ponatinib induced regression of KIT T670I tumors grown in mice. The T670I mutation is analogous to the T315I gatekeeper mutation in BCR-ABL, where it has been shown previously that the unique triple bond linker of ponatinib, in conjunction with its overall binding mode, is able to significantly reduce the steric clash with a larger, mutant isoleucine residue (18).

KIT A-loop (exons 17 and 18) mutations cause clinical resistance to imatinib and sunitinib, and these effects were recapitulated in our preclinical studies. In contrast, ponatinib had substantial potency against all 6 KIT A-loop mutants tested in Ba/F3 assays, with $IC_{50} \leq 13$ nmol/L in the background of an exon 11 primary mutation. Ponatinib likewise induced tumor regression in a Ba/F3 xenograft with a D816H mutation and induced complete and durable regression in a GIST patient-derived xenograft model with a Y823D mutation. It is predicted that mutations in the A-loop can impair binding of ponatinib, as well as imatinib and sunitinib, by destabilizing the A-loop conformation, thereby disrupting contacts between F811, at the base of the A-loop, and each of the TKIs. We hypothesize that the relatively small impact of A-loop mutations on ponatinib potency is due to the presence of an overall extended

network of optimized contacts between ponatinib and KIT throughout the kinase domain, making it less dependent than imatinib and sunitinib on interactions with F811. Importantly, however, certain mutations in the A-loop that have strong effects on all other TKIs, such as N822K, do not appear to have any effect on ponatinib potency. The basis for this is not yet understood.

Using an unbiased *in vitro* mutagenesis screen that successfully identified multiple secondary mutations that confer clinical resistance to imatinib (in the ATP pocket and A-loop) and sunitinib (in the A-loop), V654A was identified as the mutation that conferred greatest resistance to ponatinib. In Ba/F3 cells expressing a KIT exon 11 primary mutation, 40 nmol/L ponatinib suppressed emergence of all mutations except for V654A, including those in the A-loop, and 80 nmol/L ponatinib suppressed emergence of all mutations, including V654A. In similar studies using Ba/F3 cells expressing BCR-ABL, 40 nmol/L ponatinib suppressed emergence of all secondary mutations, including T315I (18). Importantly, trough concentrations of ponatinib exceed 40 nmol/L in patients dosed at 30 mg and at the recommended phase II dose of 45 mg (16). In a phase II study in patients with CML, no single mutation has been identified that consistently confers primary or secondary resistance to ponatinib (17).

Thus, these results suggest that, at clinically achievable concentrations, ponatinib has a broad inhibitory profile against KIT, with strong potency predicted against KIT with primary mutations in exon 11 coupled with most secondary mutations, including those in the A-loop and the T670I gatekeeper residue. Reduced efficacy is predicted against KIT with secondary mutation V654A or with primary activating mutation in exon 9.

The clinical activity of ponatinib was examined in 3 patients with GIST using a 30-mg, once-daily oral regimen. These patients had previously received at least 4 TKI regimens that included all 3 approved agents at standard doses plus high-dose imatinib (800 mg) and 2 of the patients had also received additional TKIs. All patients had GISTs with KIT exon 11 primary mutations. Importantly, after 4 weeks of treatment, evidence of tumor regression was observed in 2 of the 3 patients, with one patient exhibiting a response in all lesions and the second having a mixture of tumor regression and stable disease. The basis for the lack of response in the third patient is unclear.

Overall, the degree of clinical activity observed across the 3 heavily pretreated patients with GIST in this report is consistent with the broad, but not pan-KIT-inhibitory profile of ponatinib in preclinical studies. Coupled with the recent report of ponatinib activity in 2 patients with cholangiocarcinoma harboring activating FGFR fusions (34), another target of ponatinib, these results provide important support for the clinical potential of ponatinib in solid tumors with targets that are inhibited in preclinical assays with potency comparable with that of BCR-ABL. Ponatinib also potently inhibits other targets, including members of the VEGFR, PDGFR, and SRC families of kinases, which could also potentially contribute to the

efficacy observed, while also providing opportunities for treatment of patients with other activating mutations in GIST (e.g., PDGFRA).

Ponatinib is reported to be associated with the occurrence of arterial thrombotic events in heavily pretreated patients with CML and Philadelphia-positive acute lymphoblastic leukemia (ALL; ref. 17). The clinical experience with 3 patients, reported here, included one event of myocardial infarction observed after ponatinib was discontinued in a patient with severe cardiovascular risk factors. While the event was deemed unrelated by the treating physician, a contribution from ponatinib cannot be ruled out. The efficacy and safety profile of ponatinib in patients with refractory GIST is currently being examined in a phase II trial (NCT01874665), which includes molecular analyses that will allow a more precise assessment of the activity of ponatinib against specific KIT mutants, including those currently not addressed by available therapies.

Disclosure of Potential Conflicts of Interest

J.M. Gozgit, T. Zhou, S. Wardwell, Y. Ning, Y. Song, A. Kohlmann, T. Clackson, and V. M. Rivera are employees of and have ownership interest (including patents) in ARIAD Pharmaceuticals. A.P. Garner and S. Vodala have ownership interest (including patents) in ARIAD Pharmaceuticals. M.C. Heinrich reports receiving a commercial research grant from ARIAD Pharmaceuticals, has ownership interest (including patents) in MolecularMD, and is a consultant/advisory board member for ARIAD Pharmaceuticals, MolecularMD, Novartis, and Pfizer. J.A. Fletcher reports receiving speakers bureau honoraria from Novartis and is a consultant/advisory board member for ARIAD Pharmaceuticals, Bayer, and Novartis. S. Bauer is a consultant/advisory board member for GIST. No potential conflicts of interest were disclosed by the other authors.

Disclaimer

Structural coordinates for the KIT/ponatinib complex have been deposited in the Research Collaboratory for Structural Bioinformatics (RCSB) Protein Data Bank and can be accessed with the identifier 4U0I.

Authors' Contributions

Conception and design: A.P. Garner, J.M. Gozgit, R. Anjum, S. Vodala, A. Schrock, F. Wang, M.C. Heinrich, J.A. Fletcher, S. Bauer, V.M. Rivera

Development of methodology: A.P. Garner, J.M. Gozgit, R. Anjum, S. Vodala, A. Schrock, C. Serrano, M.C. Heinrich, J.A. Fletcher, S. Bauer, V.M. Rivera

Acquisition of data (provided animals, acquired and managed patients, provided facilities, etc.): A.P. Garner, R. Anjum, S. Vodala, A. Schrock, T. Zhou, G. Eilers, M. Zhu, S. Wardwell, Y. Ning, Y. Song, M.C. Heinrich, J.A. Fletcher, S. Bauer

Analysis and interpretation of data (e.g., statistical analysis, biostatistics, computational analysis): A.P. Garner, J.M. Gozgit, R. Anjum, S. Vodala, A. Schrock, T. Zhou, G. Eilers, M. Zhu, S. Wardwell, A. Kohlmann, M.C. Heinrich, J.A. Fletcher, S. Bauer, V.M. Rivera

Writing, review, and/or revision of the manuscript: A.P. Garner, J.M. Gozgit, S. Vodala, A. Schrock, T. Zhou, S. Wardwell, T. Clackson, M.C. Heinrich, J.A. Fletcher, S. Bauer, V.M. Rivera

Administrative, technical, or material support (i.e., reporting or organizing data, constructing databases): A.P. Garner, J.M. Gozgit, J. Ketzner, S. Wardwell, A. Kohlmann, J.A. Fletcher

Study supervision: A.P. Garner, J.M. Gozgit, F. Wang, T. Clackson, J.A. Fletcher, V.M. Rivera

Other (determined the co-crystal structure of KIT with ponatinib and provided structural data interpretation): T. Zhou

Acknowledgments

The authors thank T. Taguchi (Kochi Medical School, Nankoku-shi, Kochi, Japan) for the GIST-T1 cell line and X. Zhu and D. Dalgarno (ARIAD Pharmaceuticals) for assistance with structural analysis.

Grant Support

This work was supported by grants from Deutsche Krebshilfe (S. Bauer); the U.S. NIH, including 1P50CA127003-07 and 1P50CA168512-01 (J.A. Fletcher); the Virginia and Daniel K. Ludwig Trust for Cancer Research (J.A. Fletcher); the GIST Cancer Research Fund (M.C. Heinrich, J.A. Fletcher); the Life Raft Group (M.C. Heinrich, J.A. Fletcher, S. Bauer); an ASCO Young Investigator Award (C. Serrano); the Spanish Society of Medical Oncology Translational

Award (C. Serrano); and a VA Merit Award Grant (M.C. Heinrich) from the Department of Veterans Affairs.

The costs of publication of this article were defrayed in part by the payment of page charges. This article must therefore be hereby marked *advertisement* in accordance with 18 U.S.C. Section 1734 solely to indicate this fact.

Received May 30, 2014; revised August 12, 2014; accepted August 15, 2014; published OnlineFirst September 19, 2014.

References

- Heinrich MC, Corless CL, Duensing A, McGreevey L, Chen CJ, Joseph N, et al. PDGFRA activating mutations in gastrointestinal stromal tumors. *Science* 2003;299:708–10.
- Hirota S, Isozaki K, Moriyama Y, Hashimoto K, Nishida T, Ishiguro S, et al. Gain-of-function mutations of c-kit in human gastrointestinal stromal tumors. *Science* 1998;279:577–80.
- Corless CL, Barnett CM, Heinrich MC. Gastrointestinal stromal tumours: origin and molecular oncology. *Nat Rev Cancer* 2011;11:865–78.
- Heinrich MC, Griffith DJ, Druker BJ, Wait CL, Ott KA, Ziegler AJ. Inhibition of c-kit receptor tyrosine kinase activity by STI 571, a selective tyrosine kinase inhibitor. *Blood* 2000;96:925–32.
- Tuveson DA, Willis NA, Jacks T, Griffin JD, Singer S, Fletcher CD, et al. STI571 inactivation of the gastrointestinal stromal tumor c-KIT oncoprotein: biological and clinical implications. *Oncogene* 2001;20:5054–8.
- Demetri GD, von Mehren M, Blanke CD, Van den Abbeele AD, Eisenberg B, Roberts PJ, et al. Efficacy and safety of imatinib mesylate in advanced gastrointestinal stromal tumors. *N Engl J Med* 2002;347:472–80.
- Chen LL, Trent JC, Wu EF, Fuller GN, Ramdas L, Zhang W, et al. A missense mutation in KIT kinase domain 1 correlates with imatinib resistance in gastrointestinal stromal tumors. *Cancer Res* 2004;64:5913–9.
- Wardelmann E, Merkelbach-Bruse S, Pauls K, Thomas N, Schildhaus HU, Heinicke T, et al. Polyclonal evolution of multiple secondary KIT mutations in gastrointestinal stromal tumors under treatment with imatinib mesylate. *Clin Cancer Res* 2006;12:1743–9.
- Heinrich MC, Corless CL, Blanke CD, Demetri GD, Joensuu H, Roberts PJ, et al. Molecular correlates of imatinib resistance in gastrointestinal stromal tumors. *J Clin Oncol* 2006;24:4764–74.
- Heinrich MC, Maki RG, Corless CL, Antonescu CR, Harlow A, Griffith D, et al. Primary and secondary kinase genotypes correlate with the biological and clinical activity of sunitinib in imatinib-resistant gastrointestinal stromal tumor. *J Clin Oncol* 2008;26:5352–9.
- Demetri GD, van Oosterom AT, Garrett CR, Blackstein ME, Shah MH, Verweij J, et al. Efficacy and safety of sunitinib in patients with advanced gastrointestinal stromal tumour after failure of imatinib: a randomised controlled trial. *Lancet* 2006;368:1329–38.
- Nishida T, Takahashi T, Nishitani A, Doi T, Shirao K, Komatsu Y, et al. Sunitinib-resistant gastrointestinal stromal tumors harbor cis-mutations in the activation loop of the KIT gene. *Int J Clin Oncol* 2009;14:143–9.
- Demetri GD, Reichardt P, Kang YK, Blay JY, Rutkowski P, Gelderblom H, et al. Efficacy and safety of regorafenib for advanced gastrointestinal stromal tumours after failure of imatinib and sunitinib (GRID): an international, multicentre, randomised, placebo-controlled, phase 3 trial. *Lancet* 2013;381:295–302.
- George S, Wang Q, Heinrich MC, Corless CL, Zhu M, Butyrski JE, et al. Efficacy and safety of regorafenib in patients with metastatic and/or unresectable GI stromal tumor after failure of imatinib and sunitinib: a multicenter phase II trial. *J Clin Oncol* 2012;30:2401–7.
- Serrano-Garcia C, Heinrich MC, Zhu M, Raut CP, Eilers G, Ravegnini G, et al. *In vitro* and *in vivo* activity of regorafenib (REGO) in drug-resistant gastrointestinal stromal tumors (GIST). ASCO Meeting Abstracts 31:15s, 2013 (suppl; abstr 10510).
- Cortes JE, Kantarjian H, Shah NP, Bixby D, Mauro MJ, Flinn I, et al. Ponatinib in refractory Philadelphia chromosome-positive leukemias. *N Engl J Med* 2012;367:2075–88.
- Cortes JE, Kim DW, Pinilla-Ibarz J, le Coutre P, Paquette R, Chuah C, et al. A phase 2 trial of ponatinib in Philadelphia chromosome-positive leukemias. *N Engl J Med* 2013;369:1783–96.
- O'Hare T, Shakespeare WC, Zhu X, Eide CA, Rivera VM, Wang F, et al. AP24534, a pan-BCR-ABL inhibitor for chronic myeloid leukemia, potently inhibits the T315I mutant and overcomes mutation-based resistance. *Cancer Cell* 2009;16:401–12.
- Gozgit JM, Wong MJ, Wardwell S, Tyner JW, Loriaux MM, Mohammad QK, et al. Potent activity of ponatinib (AP24534) in models of FLT3-driven acute myeloid leukemia and other hematologic malignancies. *Mol Cancer Ther* 2011;10:1028–35.
- Zhang S, Wang F, Keats J, Zhu X, Ning Y, Wardwell SD, et al. Crizotinib-resistant mutants of EML4-ALK identified through an accelerated mutagenesis screen. *Chem Biol Drug Des* 2011;78:999–1005.
- Bauer S, Yu LK, Demetri GD, Fletcher JA. Heat shock protein 90 inhibition in imatinib-resistant gastrointestinal stromal tumor. *Cancer Res* 2006;66:9153–61.
- Gajiwala KS, Wu JC, Christensen J, Deshmukh GD, Diehl W, DiNitto JP, et al. KIT kinase mutants show unique mechanisms of drug resistance to imatinib and sunitinib in gastrointestinal stromal tumor patients. *Proc Natl Acad Sci U S A* 2009;106:1542–7.
- Heinrich MC, Marino-Enriquez A, Presnell A, Donsky RS, Griffith DJ, McKinley A, et al. Sorafenib inhibits many kinase mutations associated with drug-resistant gastrointestinal stromal tumors. *Mol Cancer Ther* 2012;11:1770–80.
- Guo T, Hajdu M, Agaram NP, Shinoda H, Veach D, Clarkson BD, et al. Mechanisms of sunitinib resistance in gastrointestinal stromal tumors harboring KITAY502-3ins mutation: an *in vitro* mutagenesis screen for drug resistance. *Clin Cancer Res* 2009;15:6862–70.
- Mol CD, Dougan DR, Schneider TR, Skene RJ, Kraus ML, Scheibe DN, et al. Structural basis for the autoinhibition and STI-571 inhibition of c-KIT tyrosine kinase. *J Biol Chem* 2004;279:31655–63.
- DiNitto JP, Wu JC. Molecular mechanisms of drug resistance in tyrosine kinases cAbl and cKit. *Crit Rev Biochem Mol Biol* 2011;46:295–309.
- Kantarjian H, Giles F, Wunderle L, Bhalra K, O'Brien S, Wassmann B, et al. Nilotinib in imatinib-resistant CML and Philadelphia chromosome-positive ALL. *N Engl J Med* 2006;354:2542–51.
- Talpa M, Shah NP, Kantarjian H, Donato N, Nicoll J, Paquette R, et al. Dasatinib in imatinib-resistant Philadelphia chromosome-positive leukemias. *N Engl J Med* 2006;354:2531–41.
- Kantarjian H, Shah NP, Hochhaus A, Cortes J, Shah S, Ayala M, et al. Dasatinib versus imatinib in newly diagnosed chronic-phase chronic myeloid leukemia. *N Engl J Med* 2010;362:2260–70.
- Saglio G, Kim DW, Issaragrisil S, le Coutre P, Etienne G, Lobo C, et al. Nilotinib versus imatinib for newly diagnosed chronic myeloid leukemia. *N Engl J Med* 2010;362:2251–9.
- Soverini S, Branford S, Nicolini FE, Talpa M, Deininger MW, Martinelli G, et al. Implications of BCR-ABL1 kinase domain-mediated resistance in chronic myeloid leukemia. *Leuk Res* 2014;38:10–20.
- Bradeen HA, Eide CA, O'Hare T, Johnson KJ, Willis SG, Lee FY, et al. Comparison of imatinib mesylate, dasatinib (BMS-354825), and nilotinib (AMN107) in an N-ethyl-N-nitrosourea (ENU)-based mutagenesis screen: high efficacy of drug combinations. *Blood* 2006;108:2332–8.
- Liegl B, Kepten I, Le C, Zhu M, Demetri GD, Heinrich MC, et al. Heterogeneity of kinase inhibitor resistance mechanisms in GIST. *J Pathol* 2008;216:64–74.
- Borad MJ, Champion MD, Egan JB, Liang WS, Fonseca R, Bryce AH, et al. Integrated genomic characterization reveals novel, therapeutically relevant drug targets in FGFR and EGFR pathways in sporadic intrahepatic cholangiocarcinoma. *PLoS Genet* 2014;10:e1004135.

Clinical Cancer Research

Ponatinib Inhibits Polyclonal Drug-Resistant KIT Oncoproteins and Shows Therapeutic Potential in Heavily Pretreated Gastrointestinal Stromal Tumor (GIST) Patients

Andrew P. Garner, Joseph M. Gozgit, Rana Anjum, et al.

Clin Cancer Res 2014;20:5745-5755. Published OnlineFirst September 19, 2014.

Updated version Access the most recent version of this article at:
doi:[10.1158/1078-0432.CCR-14-1397](https://doi.org/10.1158/1078-0432.CCR-14-1397)

Supplementary Material Access the most recent supplemental material at:
<http://clincancerres.aacrjournals.org/content/suppl/2014/09/20/1078-0432.CCR-14-1397.DC1>

Cited articles This article cites 33 articles, 15 of which you can access for free at:
<http://clincancerres.aacrjournals.org/content/20/22/5745.full#ref-list-1>

Citing articles This article has been cited by 11 HighWire-hosted articles. Access the articles at:
<http://clincancerres.aacrjournals.org/content/20/22/5745.full#related-urls>

E-mail alerts [Sign up to receive free email-alerts](#) related to this article or journal.

Reprints and Subscriptions To order reprints of this article or to subscribe to the journal, contact the AACR Publications Department at pubs@aacr.org.

Permissions To request permission to re-use all or part of this article, use this link
<http://clincancerres.aacrjournals.org/content/20/22/5745>.
Click on "Request Permissions" which will take you to the Copyright Clearance Center's (CCC) Rightslink site.